



POLITECNICO DI TORINO  
Repository ISTITUZIONALE

Clustering of plumes in turbulent convection

*Original*

Clustering of plumes in turbulent convection / Parodi, A; von Hardenberg, J; Passoni, G; Provenzale, A; Spiegel, EA. - In: PHYSICAL REVIEW LETTERS. - ISSN 0031-9007. - 92:19(2004). [10.1103/PhysRevLett.92.194503]

*Availability:*

This version is available at: 11583/2815078 since: 2020-04-22T14:55:44Z

*Publisher:*

AMER PHYSICAL SOC

*Published*

DOI:10.1103/PhysRevLett.92.194503

*Terms of use:*

openAccess

This article is made available under terms and conditions as specified in the corresponding bibliographic description in the repository

*Publisher copyright*

(Article begins on next page)

## Clustering of Plumes in Turbulent Convection

Antonio Parodi and Jost von Hardenberg

*CIMA, Savona and DIAM, Università di Genova, Genova, Italy*

Giuseppe Passoni

*DIAR, Politecnico di Milano, Milano, Italy*

Antonello Provenzale

*ISAC-CNR, Torino and CIMA, Savona, Italy*

Edward A Spiegel

*Department of Astronomy, Columbia University, New York, New York 10027, USA*

(Received 26 September 2003; published 14 May 2004)

Turbulent Rayleigh-Bénard convection produces fields of intense updrafts and downdrafts that are responsible for much of the vertical heat transport. These structures, called plumes or thermals, have horizontal scales comparable to the thicknesses of the boundary layers in which they arise. In the three-dimensional numerical simulations reported here, we have observed that convective plumes organize themselves into clusters with horizontal scales that grow with time and reach the width of the computational domain. In this two-scale process, kinetic energy is transferred mainly to low horizontal wave numbers while the sizes of individual plumes remain on the scale of the boundary layer thickness.

DOI: 10.1103/PhysRevLett.92.194503

PACS numbers: 47.27.Te, 92.60.Ek

In highly unstable conditions, convective overturning is dominated by isolated coherent structures, called thermals or plumes [1,2], that mix the fluid and enhance turbulent heat transfer. In many natural occurrences of turbulent convection, the plumes are observed to cluster into structures of larger scale. In rain storms, individual convective rain cells form mesoscale clusters [3]. In the intense convection in the solar atmosphere granules—the smallest resolved convective elements—cluster into mesogranules and are swept toward the edges of yet larger structures called supergranules [4]. Experiments in confined boxes also reveal the formation of large-scale order in the onset of horizontal circulations on the scale of the container [5–12], low-frequency oscillations in the temperature field [6,13,14], and clustering of convective plumes [11,14,15].

Here, we report on a numerical simulation of turbulent convection that leads to such large-scale order by the clustering of convective plumes having like signs of temperature perturbation. We present both qualitative and quantitative evidence for the occurrence of this process at a moderately large aspect ratio with periodic boundary conditions in the horizontal directions. Our horizontal boundary conditions do not, of course, apply to the closed containers used in some controlled laboratory experiments, though experiments in a circular annulus would capture aspects of the periodic boundary conditions.

The simulations reported here were performed for a fluid with a three-dimensional, solenoidal velocity field  $\mathbf{u}(\mathbf{x}, t) \equiv (u, v, w)$  and temperature field  $T(\mathbf{x}, t)$  where  $z$  is the vertical coordinate,  $w$  is the vertical velocity and  $\Delta T$

is the imposed temperature difference across the layer. As units of length and time we adopt the layer thickness,  $d$ , and the dynamical (or convective) time,  $\tau_{\text{dyn}} = \sqrt{d/g\alpha\Delta T}$  where  $g$  is the acceleration of gravity and  $\alpha$  is the coefficient of thermal expansion. Velocity is measured in units of  $d/\tau_{\text{dyn}}$  and temperature in units of  $\Delta T$ . The thermal time is  $\tau_{\kappa} = d^2/\kappa$  and the viscous time is  $\tau_{\nu} = d^2/\nu$ . A convenient measure of the overall dissipation time is the geometric mean,  $\tau_{\text{diss}} = d^2/\sqrt{\kappa\nu}$ . The main control parameters in this problem are the Prandtl number,  $\sigma = \tau_{\kappa}/\tau_{\nu}$ , and the Rayleigh number,  $R = (\tau_{\text{diss}}/\tau_{\text{dyn}})^2$ . The Boussinesq approximation is adopted throughout this work [16].

The basic equations of the system are

$$\frac{\partial \mathbf{u}}{\partial t} + \mathbf{u} \cdot \nabla \mathbf{u} = -\nabla p + T \hat{\mathbf{z}} + \left(\frac{\sigma}{R}\right)^{1/2} \nabla^2 \mathbf{u}, \quad (1)$$

$$\nabla \cdot \mathbf{u} = 0, \quad (2)$$

$$\frac{\partial T}{\partial t} + \mathbf{u} \cdot \nabla T = \frac{1}{(\sigma R)^{1/2}} \nabla^2 T. \quad (3)$$

The computational domain is a layer of unit thickness with a square planform of side  $L$  that provides another control parameter, the aspect ratio. The fluid velocity  $\mathbf{u}$  vanishes on  $z = 0, 1$  while  $T = 1$  on  $z = 0$  and  $T = 0$  on  $z = 1$ . As in many simulations of convection, periodic boundary conditions are imposed in the horizontal directions [17–20]; these mimic what happens in a small portion of the naturally arising spherical shells around planets and stars.

We integrate the equations using a numerical code that has been developed from a preexisting 3D spectral-finite difference Navier-Stokes solver [21]. The code is spectral in the horizontal, with 4/5 dealiasing [22], finite differencing in the vertical [23], and resolution of  $192^2$  grid points in the horizontal and 129 (unequally spaced) points along the vertical [24]. Time advancement is by a third-order fractional step method [25].

For brevity, we give an account of results from only one illustrative long run with  $\sigma = 0.71$ ,  $R = 10^7$ , and  $L = 2\pi$ . The initial conditions are provided by small-amplitude random velocity and temperature fluctuations around the equilibrium state. The convection rapidly evolves from the initial state to a turbulent regime with a well-mixed interior that occupies most of the fluid volume that separates the boundary layers formed at the lower and upper surfaces of the fluid [18]. The enhancement factor in total heat flux caused by convection is the Nusselt number,  $N = 16$ .

In the interior of the turbulent layer, the horizontally averaged temperature is nearly constant, but the full temperature field has strong fluctuations about this mean caused by intense convective plumes. In Fig. 1, we show a vertical cross section of the temperature field showing a forest of hot, rising plumes and of cold, descending plumes in the body of the fluid.

Plumes are characterized by a strong correlation between the temperature perturbation,  $\theta = T - \bar{T}$ , where  $\bar{T}(z)$  is the horizontal average of the temperature at level  $z$ , and the vertical velocity  $w$ . Operationally, we identify plumes on the midplane by thresholding the value of the turbulent heat flux,  $w\theta$  [26]. Thus, plumes correspond to local maxima of the vertical convective heat transport [17,18,27,28]: In our simulations, the structures that we identify as plumes account for 50% of the heat flux in the body of the fluid, while they occupy only about 8% of the area of the midplane. Outside the plumes, we observe only a weak correlation between temperature fluctuation and vertical velocity and a much lower kinetic energy density than that found within the plumes.

Plumes first appear as updrafts and downdrafts that are generated by instabilities in the boundary layers and erupt into the fluid interior [1] in a network of sheetlike struc-

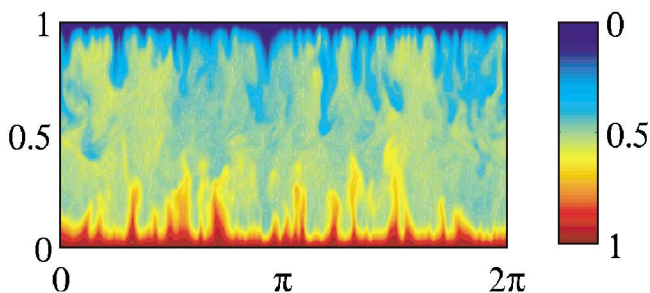


FIG. 1 (color). Vertical slice of the temperature field,  $T$ , at time  $t = 13$ .

tures. These form a spoke pattern like that observed by Busse and Whitehead [29]. At the intersections of the sheets, strongly localized structures with roughly circular horizontal cross sections form. These morph into the convective plumes whose cores have sizes comparable to the thickness of the boundary layer from which they originated. Many plumes survive the journey across the layer to arrive at the opposite boundary. There they splash down and generate the boundary layer disturbances that give rise to fresh plumes that make the return trip. The result is a statistical symmetry between rising hot plumes and descending cold plumes that reflects the basic symmetry of the Boussinesq model.

After a brief transient, the total number of convective plumes and the average area covered by each plume remains approximately constant. (In our simulation, we have an average of 110 rising and sinking plumes at each instant). Over the course of time, the spatial distribution of the ensemble of convective plumes changes dramatically from its initial statistically homogeneous array. The separation process, by which rising and sinking plumes cluster into disjoint groups, is captured by Fig. 2, showing horizontal sections of the temperature field at the midplane at two different times.

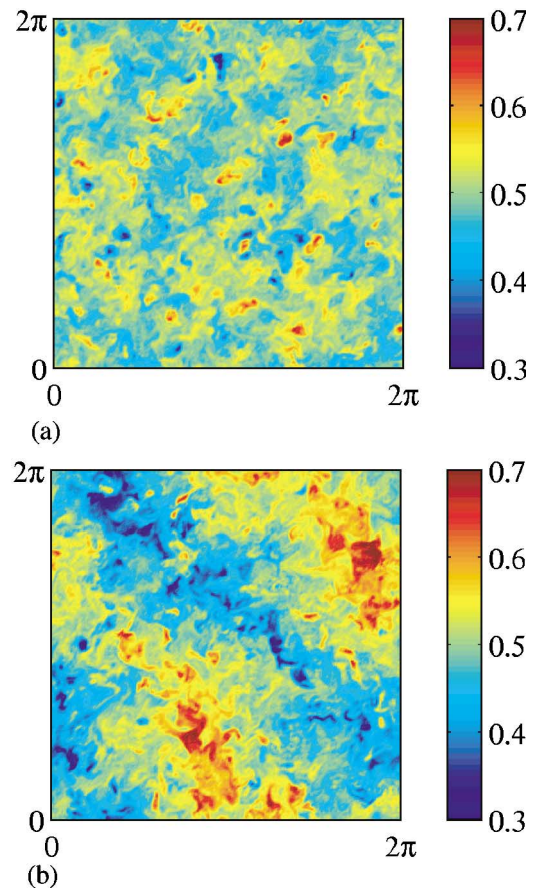


FIG. 2 (color). Horizontal slices of the temperature field,  $T$ , at the midplane,  $z = 0.5$ , at time  $t = 13$  (a) and at time  $t = 160$  (b).

At the earlier time [Fig. 2(a)], the convective plumes display a statistically homogeneous distribution. As time goes on, however, plumes of like sign cluster together to form a large-scale network [Fig. 2(b)]. Two horizontal scales thus emerge: the individual convective plumes have a mean horizontal size comparable to the boundary layer thickness, and they form clusters on the scale of the computational domain.

The process of forming structures with large horizontal scales is quantified in Fig. 3(a), showing two kinetic energy spectra  $E(k)$ , one at an early time and one later. The spectra are functions of the horizontal wave number  $k$ , each representing an average over the whole fluid column. The spectrum at late times,  $t = 160$ , shows a significantly larger energy content at small  $k$  than in the early development of the convection, at  $t = 13$ .

The kinetic energy content at the lowest wave number,  $k = 1$ , first becomes dominant at about  $t = 30$ . At this point, a two-roll circulation at the largest scale compatible with the boundary conditions,  $k = 1$ , is established [30]. After this time, the kinetic energy distribution of the

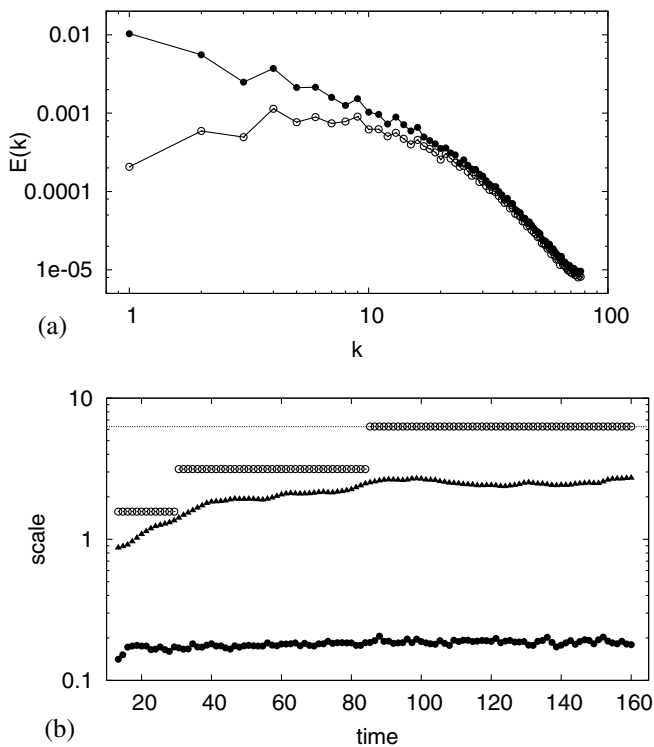


FIG. 3. (a) Total kinetic energy spectra at times  $t = 13$  (lower, dashed curve) and  $t = 160$  (upper, solid curve), as a function of the horizontal wave number  $k$ . The spectra have been averaged over three consecutive times. (b) Time evolution of the scale where the kinetic energy spectrum is maximum,  $\lambda_M$  (open circles), of the integral scale,  $\lambda_I$  (triangles), and of the average diameter of individual convective plumes (filled circles). The dashed horizontal line indicates the size of the computational domain,  $L = 2\pi$ . Time is in units of the dynamical time,  $\tau_{\text{dyn}}$ .

turbulent flow does not evolve further. In this late, statistically stationary regime, the spectrum peaks at the gravest wave number, and the dynamics may be influenced by the horizontal boundary conditions. In Fig. 3(b), we show the time evolution of the scale  $\lambda_M = 2\pi/k_M$  where the energy spectrum reaches its maximum value,  $E(k_M)$ , and of the integral scale  $\lambda_I = \int [E(k)/k] dk / \int E(k) dk$ . Also shown is the time evolution of the diameter of an individual plume. The scale where the kinetic energy spectrum is peaked,  $\lambda_M$ , and the integral scale,  $\lambda_I$ , grow with time. By contrast, the average size of the individual convective plumes remains of the order of the boundary layer thickness.

The clustering of convective plumes has been ascribed to the action of the large-scale circulation [31]. However, our results reveal that the large-scale circulation with  $k = 1$  is generated as the final stage of a process during which the energy moves slowly towards low wave numbers. This suggests the alternate view that it is the clustering of plumes that generates the large-scale wind, in agreement with the indications of recent experiments [14,15]. When the large-scale circulation is established, a positive feedback between the wind and the plumes reinforces the process.

It may be that in a further development of rectification processes, the global circulation is driven by an instability of the plumes [32]. However, inspection of the divergence field in the boundary layer suggests that at  $R = 10^7$  the clustering is due mainly to the interaction between the plumes and the boundary layers. When we initialize the system with either a pair or an ensemble of hot adjacent plumes, we see that two rising plumes of like sign in temperature perturbation weakly attract each other at very close range, but here such forces appear to be too weak to cause significant global effects. However, once plumes hit a boundary layer, they create a strong divergence of the horizontal velocity field in the boundary layer itself. This diverging horizontal velocity tends to push the roots of the newly forming plumes yet closer together, and a positive feedback is established between the pattern of convergence and divergence in the two boundary layers.

Another interesting issue with respect to large-scale circulations is that a shear mode with  $k = 0$  is not strongly excited, although such a mode is allowed by the periodic boundary conditions. This mode, found in highly truncated theoretical models for layers of infinite horizontal extent [33], has been used to rationalize the observation of large-scale wind seen in experiments [5]. Similarly, the statistical excitation of shear flows with  $k \rightarrow 0$  has been argued to be an effective process at large aspect ratios [34]. In our simulations, though such a  $k = 0$  mode is weakly generated, its amplitude remains very small, in agreement with the results reported by Hartlep *et al.* [20]. To further explore the behavior of the shear mode, we have run a few simulations that included, as

initial conditions, a vertical shear of the horizontal velocity. In all cases, the amplitude of the mode with  $k = 0$  decreased to the small values observed for the case with no initial shear.

Also of interest, is the issue of long time behavior in layers of infinite horizontal extent. Is the clustering process arrested at large but finite scale as the aspect ratio is increased, or does the clustering continue on to ever larger scales? In the latter case, convection in a layer of infinite horizontal extent may never reach a stationary state. The discussion of such issues will have to await the development of an acceptable model of this phase separation process.

We are grateful to S. Childress, C. R. Doering, L. N. Howard, and K. S. Sreenivasan for enlightening discussions and useful comments. Part of this work was done during the GFD summer program at WHOI.

- 
- [1] J. Turner, *Buoyancy Effects in Fluids* (Cambridge University Press, Cambridge, 1973).
- [2] G. Zocchi, E. Moses, and A. Libchaber, *Physica (Amsterdam)* **166A**, 387 (1990).
- [3] P. Austin and R. Houze, *J. Appl. Meteorol.* **11**, 926 (1972).
- [4] J. Zirker, *Journey from the Center of the Sun* (Princeton University Press, Princeton, NJ, 2001).
- [5] R. Krishnamurti and L. Howard, *Proc. Natl. Acad. Sci. U.S.A.* **78**, 1981 (1981).
- [6] B. Castaing, G. Gunaratne, F. Heslot, L. Kadanoff, A. Libchaber, S. Thomae, X.-Z. Wu, S. Zaleski, and G. Zannetti, *J. Fluid Mech.* **204**, 1 (1989).
- [7] J. Zhang, S. Childress, and A. Libchaber, *Phys. Fluids* **9**, 1034 (1997).
- [8] J. Zhang, S. Childress, and A. Libchaber, *Phys. Fluids* **10**, 1534 (1998).
- [9] J. Niemela, L. Skrbek, K. Sreenivasan, and R. Donnelly, *Nature (London)* **404**, 837 (2000).
- [10] J. Niemela, L. Skrbek, K. Sreenivasan, and R. Donnelly, *J. Fluid Mech.* **449**, 169 (2001).
- [11] X.-L. Qiu and P. Tong, *Phys. Rev. E* **64**, 036304 (2001).
- [12] J. Niemela and K. Sreenivasan, *Europhys. Lett.* **62**, 829 (2003).
- [13] M. Sano, X.-Z. Wu, and A. Libchaber, *Phys. Rev. A* **40**, 6421 (1989).
- [14] X.-L. Qiu and P. Tong, *Phys. Rev. E* **66**, 026308 (2002).
- [15] H.-D. Xi, S. Lam, and K.-Q. Xia, *J. Fluid Mech.* (to be published).
- [16] S. Chandrasekar, *Hydrodynamics and Hydromagnetic Stability* (Clarendon Press, New York, 1968).
- [17] C.-H. Moeng, *J. Atmos. Sci.* **41**, 2052 (1984).
- [18] R. Kerr, *J. Fluid Mech.* **310**, 139 (1996).
- [19] K. Julien, S. Legg, J. McWilliams, and J. Werne, *J. Fluid Mech.* **322**, 243 (1996).
- [20] T. Hartlep, A. Tilgner, and F. Busse, *Phys. Rev. Lett.* **91**, 064501 (2003).
- [21] G. Passoni, G. Alfonsi, and M. Galbiati, *Int. J. Numer. Methods Fluids* **38**, 1069 (2002).
- [22] G. S. Patterson and S. A. Orszag, *Phys. Fluids* **14**, 2538 (1971).
- [23] S. Sundaram and L. R. Collins, *J. Fluid Mech.* **335**, 75 (1997).
- [24] G. Grotzbach, *J. Comput. Phys.* **49**, 241 (1983).
- [25] J. Kim and P. Moin, *J. Comput. Phys.* **59**, 2 (1985).
- [26] First we detect local maxima of the turbulent heat transport field. At  $z = 0.5$ , the turbulent heat transport has average  $\langle w\theta \rangle \approx 15$  and standard deviation  $\sigma_{w\theta} \approx 30$  (at this level, temperature perturbations are order 0.1 and velocity fluctuations are order 100). We retain only those maxima in  $w\theta$  that exceed  $8\langle w\theta \rangle$ . The horizontal extent of each plume is then determined by identifying the connected region around the maximum, which has heat flux larger than  $4\langle w\theta \rangle$ . Usually, the heat flux in each plume decreases monotonically from the maximum. The number of identified plumes grows for decreasing values of the thresholds, but the temporal trends in the number and size of plumes do not change. Note, also, that the Taylor microscale for this simulation is about 0.12, about half the average horizontal size of the plume cores.
- [27] J. Deardorff, *Bound.-Layer Meteorol.* **7**, 199 (1974).
- [28] J. Werne, *Phys. Rev. E* **48**, 1020 (1993).
- [29] F. Busse and J. Whitehead, *J. Fluid Mech.* **66**, 67 (1974).
- [30] The observations of large-scale winds on the scale of the container reported in experiments refer to one single roll filling the container. The periodic boundary conditions used here do not admit a single roll. Rather, we find the pair of counterrotating rolls at late times in our simulations, when the energy has peaked at  $k = 1$ , and a large-scale circulation has been established. By contrast, in closed containers, the minimum finite wave number is  $k = 1/2$ , corresponding to the single-roll circulation.
- [31] L. Kadanoff, *Phys. Today* **54**, No. 8, 34 (2001).
- [32] S. Childress, *Chaos* **10**, 28 (2000).
- [33] L. Howard and R. Krishnamurti, *J. Fluid Mech.* **170**, 385 (1986).
- [34] T. Elperin, N. Kleorin, I. Rogachevskii, and S. Zilitinkevich, *Phys. Rev. E* **66**, 066305 (2002).